WUB-IP: A High-Precision UWB Positioning Scheme for Indoor Multi-user Applications

Zhendong Yin, *Member, IEEE,* Xu Jiang, Zhutian Yang, *Member, IEEE,* Nan Zhao, *Senior Member, IEEE,* Yunfei Chen, *Senior Member, IEEE,*

***Abstract*—High-precision positioning scheme, an important part of the indoor navigation system, can be implemented using an ultra-wide band (UWB) based ranging system. Recently, solutions for precise positioning in dense multi-path and non-line-of-sight (NLOS) conditions have attracted a lot of attention in literature. On the other hand, it is expected that Waveform Division Multiple Access (WDMA) technology for multi-user UWB positioning application will be indispensable in the near future. In this regard, a WDMA-UWB based positioning scheme is investigated in this paper, for enhancing the performance of positioning accuracy in multi-user applications. In accordance with practical requirements of indoor positioning, we propose a new indoor positioning scheme, termed as WUB-IP. This scheme adopts WDMA for multiple access, and utilizes an entropy-based approach for the Time of Arrival (TOA) estimation. Moreover, a transfer learning approach is used for ranging error mitigation in NLOS conditions, in order to improve the positioning accuracy in NLOS conditions. System-level simulations demonstrate that the proposed scheme enhances the performance of indoor positioning for multi-user applications.**

***Index Terms*—Indoor positioning, transfer learning, UWB, waveform division multiple access.**

I. Introduction

IN indoor environment is beyond the coverage of GPS. Ultra-wide band (UWB) positioning is a strong enabler for several applications in both industry and everyday life [1]–[6]. This new technology has a lot of advantages over traditional techniques, such as GPS and RFID, as it has the capability of high precision ranging in a small indoor area due to high-temporal resolution and good obstacle-penetration capabilities [7]–[10]. Nowadays, UWB positioning has been regarded as a potential solution for high precision requirements, such as equipment and personnel tracking, asset management in warehouse, and home monitoring [11], [12].

One key element of the indoor UWB positioning system is ranging, which is mainly dependant on the time of arrival (TOA) estimation [13]. There exist some critical challenges for TOA estimation, such as electronic jamming, dense multipath, and non-line-of-sight (NLOS) conditions [14], [15]. In electromagnetic environments (such as crowded buildings), various wireless signals may interfere with the reception of UWB pulses. Furthermore, dense multi-path and NLOS conditions are critical for FP detection, and thereby, degrade ranging and localization performances [16]. Consequently, for high-precision FP detection, several maximum energy-based approaches are under consideration, such as maximum energy selection (MES), MES searching-back (MES-SB), coherent detection and threshold crossing based methods [17]. Additionally, statistical analysis approaches are also utilized for range information model construction [16]. However, the delay between FP and the strongest path (SP) in NLOS conditions is a challenge for TOA estimation.

On the other hand, the requirement for multi-user application still exists. Multiple access technology for UWB communication has been an important topic in UWB research for a long time. Time hopping UWB (TH-UWB) and direct sequence UWB (DS-UWB) are two main approaches for UWB multiple access, which utilize PN codes to distinguish users. Unfortunately, these two approaches are inefficient for UWB pulse-based ranging in a multi-user application, especially in dense multi-path conditions. In this regard, a more efficient scheme for UWB multiple access is proposed in [18] and [19], namely, waveform division multiple access (WDMA). In WDMA-UWB, orthogonal waveforms are used for multiple access by using appropriate waveform design, which releases the limitations to communication and spectrum efficiency. Furthermore, WDMA-UWB is suitable for multi-user ranging application in dense multi-path conditions, due to the waveform orthogonality. Therefore, WDMA-UWB is viewed as a novel approach to address the multiple access interference issue in indoor high-precision positioning systems.

Although there have been several excellent works on UWB positioning and WDMA-UWB, these two important areas are usually studied separately in the literature. However, it is of great importance to combine them for even greater benefits. Thus, the key objective of this paper is to propose a novel high-precision indoor positioning scheme based on WDMA-UWB ranging, in order to enhance the location accuracy for the multi-user application requirement in indoor harsh environments. The key contributions are stated as follows.

- In this research, the high-precision positioning scheme is proposed for multiple users in indoor harsh environments. In places with complex electromagnetic, such as offices, the reception of UWB pulses will be interfered by various signals. Furthermore, the asynchronization among users may intensify MAI. In this regard, we propose an effective scheme to enhance the positioning accuracy, which can be a potential solution for application.

Z. Yin, X. Jiang and Z. Yang are with the School of Electronics and Information Engineering, Harbin Institute of Technology, Harbin, China.

N. Zhao is with the School of Information and Communication Engineering, Dalian University of Technology, Dalian, China

Y. Chen is with the School of Engineering, University of Warwick, Coventry CV4 7AL, U.K.

Corresponding author: Z. Yang (email: yangzhutian@hit.edu.cn)

- We propose a Coif4 wavelets-based approach for UWB pulse waveform designing, and use the WDMA-UWB scheme for improving the anti-MAI performance as well as for meeting the utility complexity requirement for application. The proposed WDMA-UWB is more effective compared to other UWB multi-access schemes.
- We develop an information entropy-based approach for FP detection, whereas the entropy is used to measure the randomness of the received signals, and the FP is detected by determining the sample with drastic entropy decreasing. This approach can improve the TOA estimation of FP in a dense multi-path condition.
- The ranging errors due to NLOS conditions are mitigated by using a transfer learning approach. In this approach, the shared-hidden-layer autoencoder (SHLA) is utilized to obtain the common knowledge among different conditions. Thereby, the ranging accuracies in NLOS conditions can be improved.
- The proposed scheme is termed as WUB-IP (WDMA-UWB Based Indoor Positioning). We conduct a system level performance evaluation of WUB-IP and compare it with other indoor positioning approaches in terms of key performance metrics.

The rest of the paper is organized as follows. Section II presents the underlying system model of WUB-IP. The WUB-IP positioning framework is introduced in Section III, followed by the performance evaluation in Section IV. Finally the paper is concluded in Section V.

II. System Model

We consider a UWB-based indoor positioning system, which adopts the round-trip time-of-flight (RTOF) measurement for ranging. We assume M stationary base stations (BSs) with known locations and N users with positioning requirements in an indoor region. Users make positioning requests by sending pulses to BSs, receive the response signals from BSs. By estimating RTOF, users calculate the distances from BSs, and thereby, position themselves. The system is shown in Fig. 1.

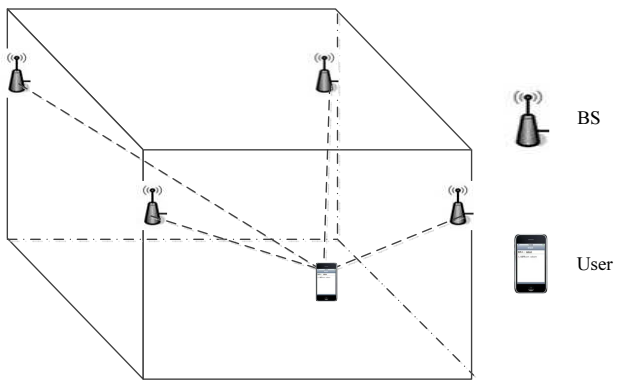

Fig. 1. Illustration of the indoor positioning system (e.g., 4 BSs and 1 user).

For each user, the position can be estimated as follows:

$$\begin{cases} \sqrt{(X_1-X)^2+(Y_1-Y)^2+(Z_1-Z)^2}=d_1 \\ \sqrt{(X_2-X)^2+(Y_2-Y)^2+(Z_2-Z)^2}=d_2 \\ \cdots \\ \sqrt{(X_M-X)^2+(Y_M-Y)^2+(Z_M-Z)^2}=d_M \end{cases}, \quad (1)$$

where $\{X, Y, Z\}$ and $\{X_M, Y_M, Z_M\}$ denote the coordinates of the user and the Mth BS, respectively; d_M denotes the Euclidean distance between them.

The user position is estimated by solving

$$\min\left(\sum_{m=1}^{M}\left|\sqrt{(X-X_m)^2+(Y-Y_m)^2+(Z-Z_m)^2}\right|-\hat{d}_m\right), \quad (2)$$

where $\hat{d}_m$ denotes the estimated distance between the user and the mth BS. In this research, the optimization problem is solved by using least squares error and Taylor series expansion (LSE-Taylor).

Communications between users and BSs are based on WDMA-UWB, and the frequency of UWB ranges between 2 GHz to 10 GHz. BS transmitters employ binary phase-shift key (BPSK) modulation for information transmission. For each transmitter, WDMA-UWB is used for the multi-user service. Therefore, a data packet with a size of P bits transmitted by each transmitter for ranging the nth-user is given by

$$x_n(t)=\sum_{p=1}^{P} b_k(p)\,\omega_n(t-pT_s), \quad (3)$$

where $b_k(i)$ and T_s denote the BPSK symbols and its duration, respectively; ω_n denotes the UWB pulse waveform for the nth user. The signal transmitted for all users is given by

$$s(t)=\sum_{n=1}^{N} x_n(t), \quad (4)$$

We assume densely multipath channel for the UWB ranging system. Both line-of-sight (LOS) and non-line-of-sight (NLOS) models are included. Consequently, models CM1 to CM4 in IEEE802.15.4a standard are adopted, and the channel impulse response is given by

$$h(t)=\sum_{l=0}^{L}\sum_{k=0}^{K}\alpha_{k,l}\exp(j\phi_{k,l})\delta(t-T_l-\tau_{k,l}), \quad (5)$$

where $\alpha_{k,l}$ denotes the gain of the kth path component in the lth cluster, T_l denotes the time delay of the lth cluster, $\tau_{k,l}$ denotes the time delay of the kth multipath component in the lth cluster, phase $\phi_{k,l}$ is distributed uniformly in $[0, 2\pi)$, and L denotes the number of clusters.

The received signal can be given by

$$r(t)=\sum_{l=0}^{L}\sum_{k=0}^{K}\alpha_{k,l}\exp(j\phi_{k,l})s(t-T_l-\tau_{k,l})+n(t)+i(t), \quad (6)$$

where $i(t)$ denotes the multi-access interference signal.

Then the specific signal waveform is separated from the receive signal by using a match-filter, and used to measure RTOF.

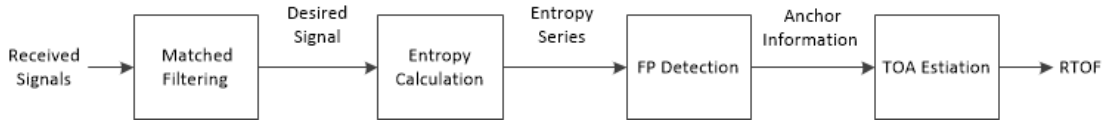

Fig. 2. The procedure of FP detection based on entropy decreasing.

III. WUB-IP Framework

In this section, we introduced the framework of our proposed scheme for indoor high-precision positioning, i.e., Waveform Division Multiple Access-UWB Based Indoor Positioning (WUB-IP). The objective of WUB-IP is to enhance the positioning accuracy for multi-user localization applications in harsh indoor environments.

A. Design of Pulse Waveform

In WDMA-UWB communication system, each user is assigned a specific waveform as the message symbol. These pulse waveforms are particularly designed to be orthogonal to each other, in order to avoid the multiple access interference between users. Therefore, the pulse waveform design is the key procedure for WDMA-UWB communication system. As analyzed in [18], Coiflet wavelets has good performances in mutual correlation. Therefore, we adopt Coiflet wavelets for UWB pulse waveform designing, which is shown as follows

$$\psi_{a,b}(t) = |a|^{-\frac{1}{2}} \psi\left(\frac{t-b}{a}\right), \tag{7}$$

where ψ denotes the basic wavelets function. In this research, we choose Coif4 wavelets as the basic wavelet function.

The nth user is allocated with a specific wavelet, which is given by

$$\psi^n(t) = \psi_{n,0}(t) - \psi_{0,n}(t). \tag{8}$$

The cross-correlation between waveforms of nth user and mth user is given by (9). Due to the orthogonality of Coiflets, different users can be distinguished effectively in applications.

B. Time of arrival estimation

The RTOF-based ranging is inherently dependent on the TOA estimation. The Cramer-Rao Lower Bound (CRLB) of TOA-based ranging is given by

$$V\left\{\hat{d}\right\} \geq \sqrt{\frac{c^2}{8\pi^2 B^2 \gamma}}, \tag{10}$$

where B and γ denote the bandwidth and signal-to-noise ratio of the received signal, respectively.

As analyzed in [18], theoretical accuracy of UWB-based ranging can achieve centimeter. However, the practical ranging accuracy in applications is only at the level of decimeters, which is due to the lower FP detection accuracy. Due to dense multipath and NLOS transmission, FP may be less intense on receive signals later. Therefore, FP detection approaches based on amplitude and first-arrival will be inefficient. However, we can determine the FP by detecting the entropy changes, which can represent the degree of randomness. As a result, the FP can be determined by choosing the sample with drastic entropy decreasing. The procedure of FP detection based on entropy decreasing is illustrated in Fig. 2.

Before FP detection, the desired signal for the user ranging is detected by using matched filters (MF), whereas the filtering result for the kth path in lth cluster is given by

$$y_{k,l}(t) = \int_{nT_s+T_l+\tau_{k,l}}^{t} r_{k,l}(t)\, h_{k,l}(t-\lambda) \mathrm{d}\lambda. \tag{11}$$

In order to improve the accuracy of FP detection, the entropy of received signals is calculated. At first, we set a threshold, which ensure that desired signal pulses exceed threshold in most cases, and the noise can rarely exceed. As analyzed in [19], the threshold can be set based on the variance of received noise, which is given by

$$\eta = \alpha\sigma, \tag{12}$$

where σ and α denote the standard deviation of noise and the constant factor for threshold adjustment, respectively.

Then, define the received signals as $\mathbf{R} = [r_{n,k}]_{N\times K}$, where N and K denote the number of frames and the length of received signals, respectively. Therefore, $R_{n,k}$ denotes kth sample in the nth frame. By comparing $\mathbf{R}$ with η, the result matrix $\mathbf{RE}$ is obtained as

$$\mathbf{RE}_{n,k} = \begin{cases} 1 & if \quad \mathbf{R}_{n,k} > \eta \\ 0 & else \end{cases}. \tag{13}$$

For the kth sample, the sample before the kth index in all frames is regarded as a new sequence, and the subset $\mathbf{\Phi}_k = \{l_n\}$ can expressed as

$$\begin{aligned} l_n &= \arg\max_m m, \\ s.t. \quad &(a) \quad \mathbf{RE}_{n,m} = 1; \\ &(b) \quad m < k. \end{aligned} \tag{14}$$

Then, we get the subsets $\mathbf{\Phi}_k$ of the received signals. We let e_i be the ith non-repetitive element in $\mathbf{\Phi}_k$. Therefore, the entropy is given by

$$E_k = -\sum_{i=1}^{I} (p_i/K) \log_b (p_i/K), \tag{15}$$

where p_i denotes the occurrence frequency of e_i.

In view of information theory, the largest entropy will be achieved when all non-repetitive elements occur with the same frequency, namely, random distribution. However, for the desired signals, the corresponding entropies are relatively small, because these samples exceed threshold in most cases.

$$\begin{aligned}\langle \psi^n(t) \cdot \psi^m(t) \rangle &= \langle [\psi_{n,0}(t) - \psi_{0,n}(t)] \cdot [\psi_{m,0}(t) - \psi_{0,m}(t)] \rangle \\ &= \langle \psi_{n,0}(t) \cdot \psi_{m,0}(t) \rangle - \langle \psi_{n,0}(t) \cdot \psi_{0,m}(t) \rangle - \langle \psi_{m,0}(t) \cdot \psi_{0,n}(t) \rangle + \langle \psi_{0,n}(t) \cdot \psi_{0,m}(t) \rangle \\ &= 0 \end{aligned} \tag{9}$$

C. Ranging error mitigation

The precision of indoor positioning is mainly dependent on ranging accuracy. Due to adoption of multi-anchors, it will lead to an accumulation of ranging error for each anchor, which severely impacts the positioning precision. In order to improve the ranging accuracy under NLOS conditions, a transfer learning-based approach is adopted to mitigate the ranging error. Transfer learning was proposed to reuse the knowledge learned previously from other data [20], [21]. The idea is to utilize commonalities among different learning tasks to share statistical strength, and transfer the common knowledge across tasks [21]–[23]. In this research, the shared-hidden-layer autoencoder (SHLA) is utilized to extract the common knowledge among different conditions, and realize transfer learning.

After extracting features from received signals, two sets of data are built, i.e., training set and target set (or test set). The same features are adopted for the two sets, and the corresponding ranging error is adopted as additional feature for training samples. By training SHLA, a model for ranging error estimation is obtained, and the mitigation procedure is simply performed by $\hat{d} - \hat{\Delta}$. We utilize SHLA here to extract the common knowledge among different application scenarios (i.e., LOS of indoor residential, NLOS of indoor residential, LOS of indoor office and NLOS of indoor office). The structure of the SHLA is shown in Fig. 3, where target values are also used for input, so that common feature representations can be found for both training data and target data in an unsupervised way. In response to an input example x, the hidden representation $h(x)$ is

$$h(x) = f(W_1 x + b_1), \tag{16}$$

where $f(z)$ is a non-linear activation function, typically a Sigmoid function $f(z) = 1/(1+\exp(-z))$ applied component-wise, W_1 is a weight matrix, and b_1 is a bias vector.

The reconstruction process is completed at the network output layer, which takes the hidden representation h, and maps it back to a reconstruction (i.e., $\widetilde{x}$) as

$$\widetilde{x} = f(W_2 h(x) + b_2), \tag{17}$$

where W_2 and b_2 denote a weight matrix and a bias vector, respectively.

We note that the key element for SHLA is the sharing of same parameters for the mapping from the input layer to the hidden layer, between target samples and training samples. However, independent parameters are adopted for the reconstruction process. Therefore, for a set of training examples X_{tr}, the objective function is given by

$$\jmath_{tr}(\theta_{tr}) = \sum_{x \in \chi^{tr}} \|x - \tilde{x}\|^2. \tag{18}$$

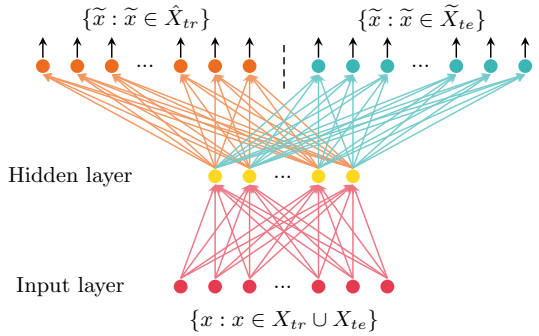

Fig. 3. Illustration of the shared-hidden-layer autoencoder (SHLA) on the training set and test set [24].

Similarly, the objective function the set of test examples X_{te} is as

$$\jmath_{te}(\theta_{te}) = \sum_{x \in \chi^{te}} \|x - \tilde{x}\|^2, \tag{19}$$

where the parameters $\theta_{tr} = \{W_1, W_2^{tr}, b_1, b_2^{tr}\}$, and $\theta_{te} = \{W_1, W_2^{te}, b_1, b_2^{te}\}$ share the same parameters $\{W_1, b_1\}$.

Then, we join the objective functions for two sets, and obtain the overall objective function as

$$\jmath_{SA}(\theta_{SA}) = \jmath_{tr}(\theta_{tr}) + \gamma \jmath_{te}(\theta_{te}), \tag{20}$$

where $\theta_{SA} = \{W_1, W_2^{tr}, W_2^{te}, b_1, b_2^{tr}, b_2^{te}\}$ are the parameters to be optimized during training, the hyper-parameter γ controls the strength of the regularization.

Training SHLA is equivalent to training a basic autoencoder, and the standard back-propagation algorithm can be applied. To minimize the objective function, the shared hidden layer is biased to make the distribution induced by the training set as similar as possible to the distribution induced by the target set. This helps to regularize the functional behavior of the autoencoder.

IV. Performance Evaluation

In this section, we evaluate the performances of WUB-IP under different scenarios. We implement WUB-IP with the topology as shown in Fig. 4. We consider a cubic region with each side of 20 meter, that is occupied by 4 BSs placed at the corners of the ceiling. The potential users are assumed to be Poisson distributed in the whole region with a mean density. The positioning requests are event-driven, and generate randomly. Four channel models mentioned above are in consideration. We compare our proposed scheme with existing approaches in the same simulation configuration.

Firstly, we evaluate the performances for FP detection of the entropy-based approach in 4 channel models. As shown in

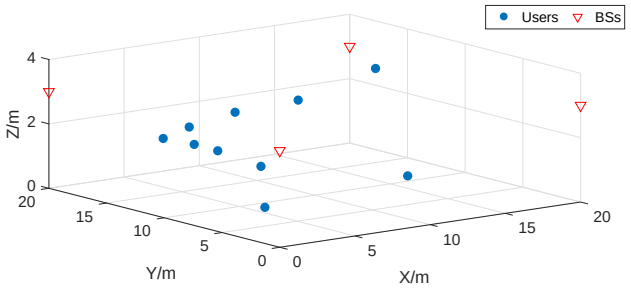

Fig. 4. Simulated user topology; The blue spots represent the locations of uses; The red triangles represent the locations of BSs.

TABLE I
FEATURES IN SIMULATION

Feature	Expression
Maximum Amplitude	$R_{max} = \max \lvert r(n) \rvert$
Energy	$E_r = \sum_n \lvert r(n) \rvert^2$
Mean Excess Delay	$\tau_m = \frac{\sum_l a_l^2 \tau_l}{\sum_l a_l^2}$
RMS Delay Spread	$\tau_{RMS} = \sqrt{\frac{\sum_k a_k^2 (\tau_k - \tau_m)^2}{\sum_k a_k^2}}$
Kurtosis	$K = \frac{E(r(n)^4)}{E^2(r(n)^2)}$
Number of Significant Paths (A)	$N_1 = \sum_n \mathrm{sgn}\left(\lvert r(n) \rvert > T\right)$
Number of Significant Paths (B)	$N_2 = \arg\min\left(E_{ce}\left(n\right)\right)$
Estimated Distance	d

Fig. 5, the entropy amplitude has a significant decline when the FP signal achieves. When SNR = 10dB, the estimated time for FP can get very close to the actual value. Especially, in CM1 and CM2, TOA estimation errors are 0.35ns and 0.47ns. In CM3 and CM4, the detection accuracies decrease, due to NLOS conditions, where TOA estimation errors are 0.77ns and 0.6ns, respectively.

Next, we evaluate the performance of ranging error mitigation. As shown in Fig. 5, ranging error under LOS conditions is much smaller than that under NLOS conditions. When other conditions are fixed, ranging error varies with SNR. Thus, the features we select should be with the capability to distinguish LOS and NLOS conditions, as well as SNR estimation capability. Meanwhile, under the LOS condition, the strongest path almost corresponds to the first path, but under the NLOS condition, some weak multipath components precede the strongest path. So mean excess delay and root-mean-square (RMS) delay spread can be selected as features because they can describe the degree of multipath of the channel. Taking all these into account, the features extracted can be summarized as shown in Table I, where $T = 10^{\frac{XdB}{20}} \max\left(\lvert r(n) \rvert\right)$ denotes the threshold, and $E_{ce}(n) > \varepsilon \cdot E_r$ denotes the cumulative energy of $r(n)$.

The ranging error mitigation is evaluated in terms of *root-mean-square error* (RMSE), with the SNR varying between -5dB and 15dB. Fig. 6 indicates that the ranging errors after mitigation are significantly lower than those without mitigation. With SNR increasing, the RMSEs of ranging decrease continually. The maximum of RMSE can be near 0.08m in LOS conditions, and 0.15m in NLOS conditions. Moreover, the RMSE of ranging with mitigation is lower than 0.03m, when SNR is higher than 5dB. Hence, we can draw the conclusion that the proposed approach is effective in harsh conditions.

We also evaluate the ranging accuracy performance by comparing with existing approaches. As shown in Fig. 7, the ranging RMSEs of all approaches and CRLB decrease as SNR increasing. The proposed approach has a better performance than existing approaches. Different from existing approaches getting to convergence early, the proposed approach gets close to the CRLB, and the ranging RMSE can achieve the centimeter level.

We evaluate the positioning accuracy performance of WUB-IP in Fig. 8. The positions of users are estimated when SNR = 10dB SNR. Taking one user for example, in each channel model, the difference between the actual position and estimated one is magnified and shown in the subfigure on top right. The positioning errors are at the level of centimeters. Particularly, in the LOS indoor residential condition, the positioning error is around 6cm. In NLOS conditions (CM2 and CM4), the positioning errors are less than 10cm. Therefore, the positioning accuracy of WUB-IP is acceptable for multi-user applications in indoor environments.

Last, we evaluate the positioning accuracy performances of WUB-IP in different SNR conditions. As shown in Fig. 9, positioning RMSE decreases with SNR increasing. RMSEs in 4 channel models can achieve less than 2cm, and especially in the LOS indoor residential condition, the RMSE is always less than 2cm, and less than 1cm in some cases. Therefore, we can draw the conclusion that the proposed indoor positioning scheme, i.e., WUB-IP, can be a promising solution for the high-precision positioning requirements in indoor harsh environments.

V. CONCLUSIONS

In this paper, a new UWB-based indoor positioning scheme, termed as WUB-IP, has been proposed for high-precision indoor positioning. WUB-IP is a specially enhanced scheme for multi-user applications, which employs WDMA for multiple access, and uses a novel UWB pulse designing. Therefore, WUB-IP has a good performance on the reliability and efficiency. It not only fulfills the practical requirements in dense multi-path conditions, but also ensures efficiency in NLOS conditions by using transfer learning. Performance evaluation shows that WUB-IP achieves a higher positioning accuracy than existing approaches in complex electromagnetic environments. Besides, WUB-IP reduces harmful interferences among users compared to TH-UWB and DS-UWB based approaches. Hence, WUB-IP provides a viable solution for practical high-precision positioning applications.

ACKNOWLEDGEMENTS

This work is supported by the National Natural Science Foundation of China (Grant No: 61471142, 61102084, 61601145 and 61571167).

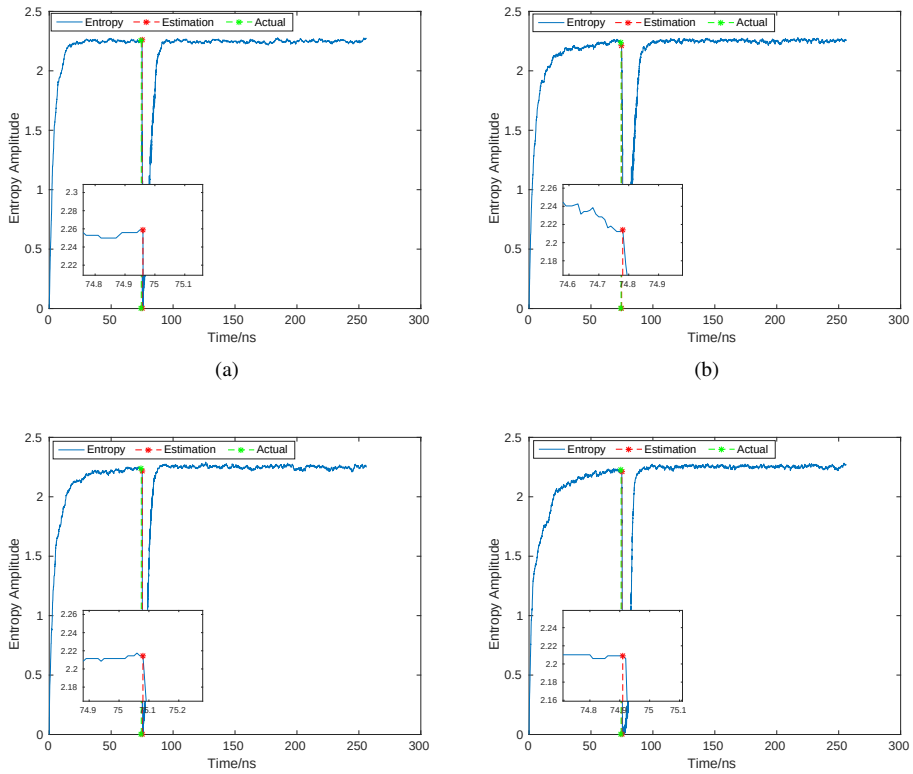

Fig. 5. FP detection performance of the entropy-based approach, (a) in CM1, (b) in CM2, (c) in CM3, (d) in CM4

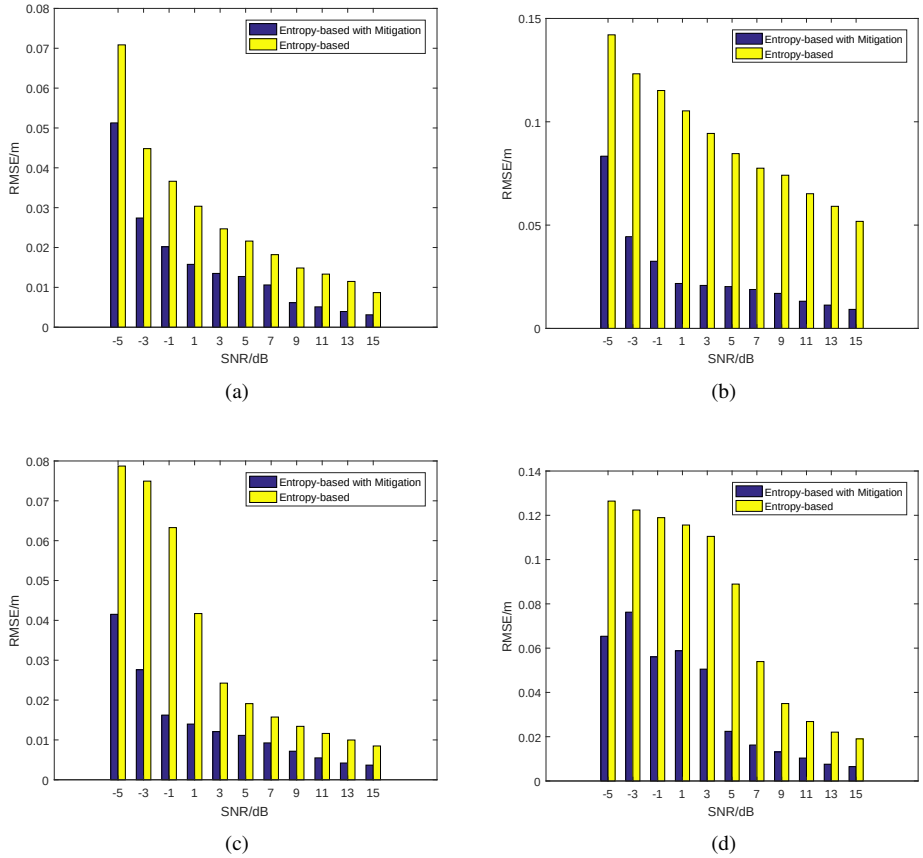

Fig. 6. Performances of ranging error mitigation, (a) in CM1, (b) in CM2, (c) in CM3, (d) in CM4

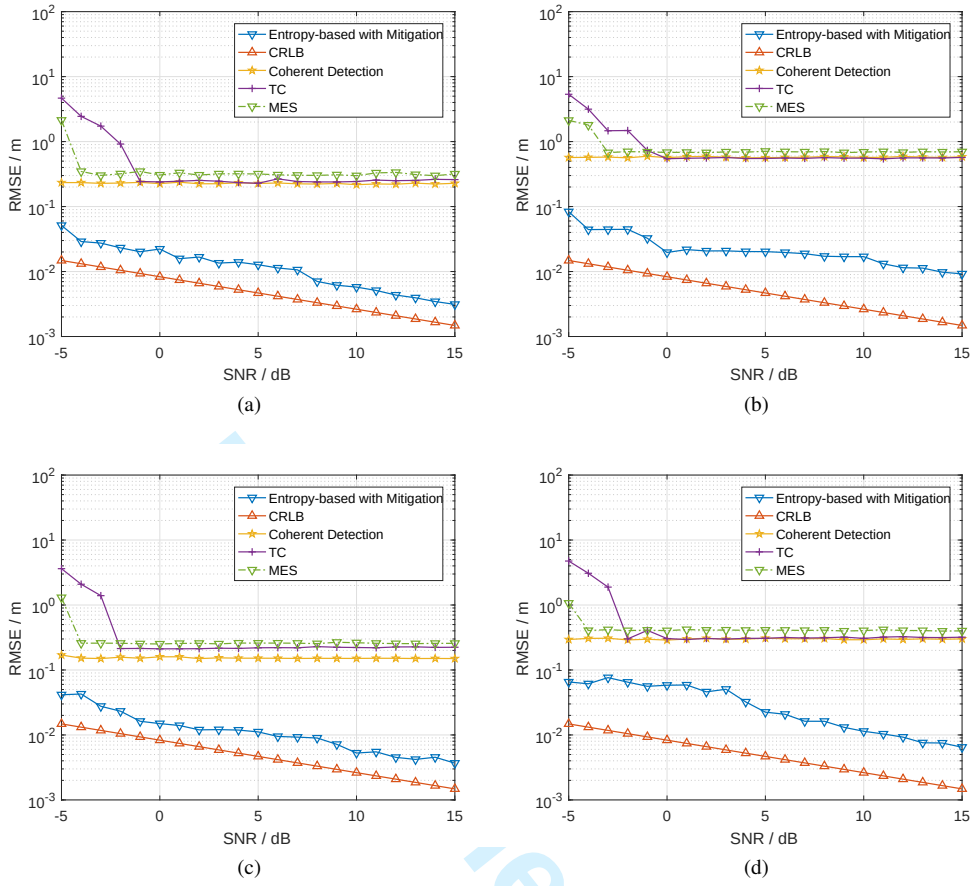

Fig. 7. Performance comparison in ranging RMSE, (a) in CM1, (b) in CM2, (c) in CM3, (d) in CM4

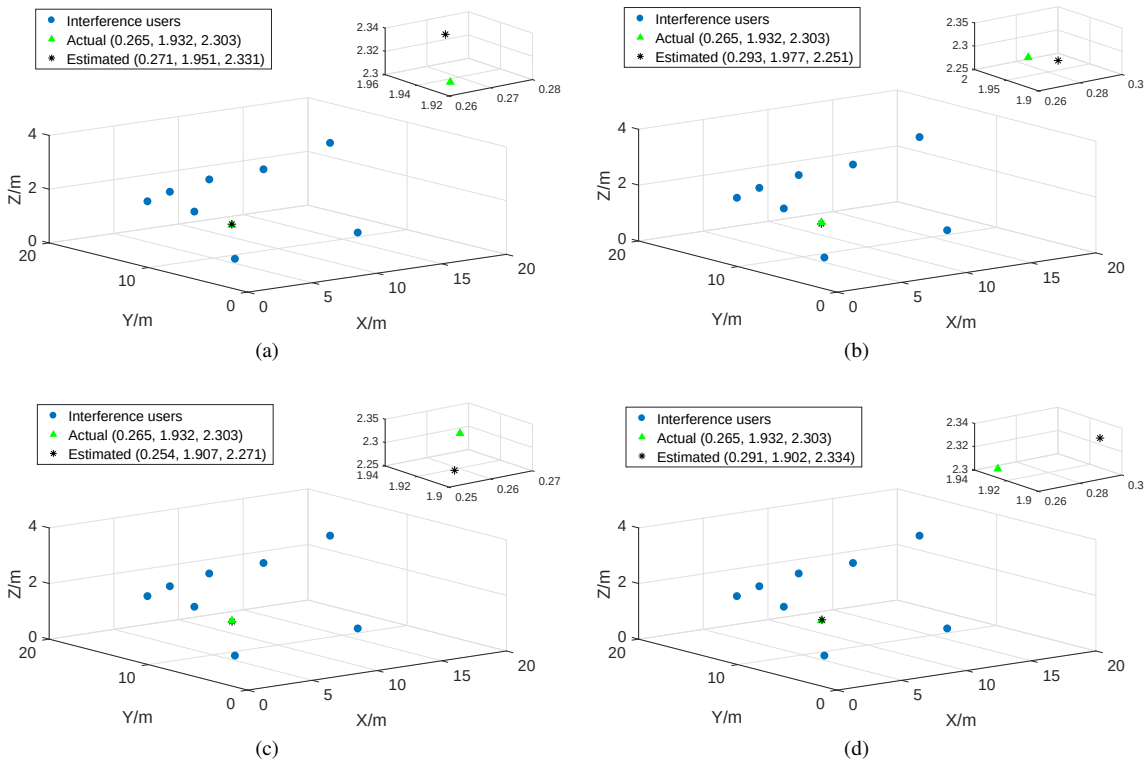

Fig. 8. Performance of positioning, (a) in CM1, (b) in CM2, (c) in CM3, (d) in CM4

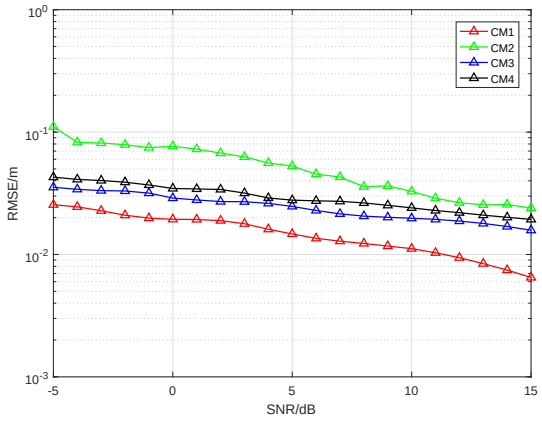

Fig. 9. Positioning accuracy comparison for WUB-IP (10000 iterations are performed, and the RMSE is obtained).

REFERENCES

[1] S. Bartoletti, M. Guerra, and A. Conti, "Uwb passive navigation in indoor environments," in *International Symposium on Applied Sciences in Biomedical and Communication Technologies*, p. 175, 2011.

[2] A. Conti, M. Guerra, D. Dardari, and N. Decarli, "Network experimentation for cooperative localization," *IEEE J. Sel. Areas Commun.*, vol. 30, no. 2, pp. 467–475, 2012.

[3] Y. Zhou, C. L. Law, Y. L. Guan, and F. Chin, "Indoor elliptical localization based on asynchronous uwb range measurement," *IEEE Trans. Instrum. Meas.*, vol. 60, no. 1, pp. 248–257, 2011.

[4] G. D. Angelis, A. Moschitta, and P. Carbone, "Positioning techniques in indoor environments based on stochastic modeling of uwb round-trip-time measurements," *IEEE Trans. Intell. Transp. Syst.*, vol. 17, no. 8, pp. 2272–2281, 2016.

[5] W. Liu, H. Ding, X. Huang, and Z. Liu, "Toa estimation in ir uwb ranging with energy detection receiver using received signal characteristics," *IEEE Commun. Lett.*, vol. 16, no. 5, pp. 738–741, 2012.

[6] J. Wang, X. Zhang, Q. Gao, H. Yue, and H. Wang, "Device-free wireless localization and activity recognition: A deep learning approach," *IEEE Trans. Veh. Technol.*, vol. PP, no. 99, pp. 1–1, 2016.

[7] M. Yasir, S. W. Ho, and B. N. Vellambi, "Indoor position tracking using multiple optical receivers," *Journal of Lightwave Technology*, vol. 34, no. 4, pp. 1166–1176, 2016.

[8] J. H. Seong, E. C. Choi, J. S. Lee, and D. H. Seo, "High-speed positioning and automatic updating technique using wi-fi and uwb in a ship," *Wireless Personal Communications*, pp. 1–17, 2016.

[9] F. Despaux, K. Jaffres-Runser, A. V. D. Bossche, and T. Val, "Accurate and platform-agnostic time-of-flight estimation in ultra-wide band," in *IEEE Pimrc*, 2016.

[10] J. Wang, X. Zhang, Q. Gao, and X. Ma, "Device-free simultaneous wireless localization and activity recognition with wavelet feature," *IEEE Trans. Veh. Technol.*, vol. 66, no. 2, pp. 1659–1669, 2017.

[11] Y. Sun, W. Meng, L. Cheng, N. Zhao, K. Zhao, and N. Zhang, "Human localization using multi-source heterogeneous data in indoor environments," *IEEE Access*, vol. PP, no. 99, pp. 1–1, 2017.

[12] J. Wang, Q. Gao, M. Pan, X. Zhang, Y. Yu, and H. Wang, "Towards accurate device-free wireless localization with a saddle surface model," *IEEE Trans. Veh. Technol.*, vol. 65, no. 8, pp. 6665–6677, 2016.

[13] J. Wang, Q. Gao, Y. Yu, X. Zhang, and X. Feng, "Time and energy efficient tof-based device-free wireless localization," *IEEE Trans. Ind. Informat.*, vol. 12, no. 1, pp. 158–168, 2016.

[14] S. Fang, B. Champagne, and I. Psaromiligkos, "Joint toa/aoa estimation of ir-uwb signals in the presence of multiuser interference," in *Proc. SPAWC'14*, pp. 504–508, 2014.

[15] S. Wei, R. Annavajjala, P. V. Orlik, A. F. Molisch, M. Ochiai, and A. Taira, "Non-coherent toa estimation for uwb multipath channels using max-eigenvalue detection," in *Proc. ICC'12*, pp. 4509–4514, 2012.

[16] S. Bartoletti, W. Dai, A. Conti, and M. Z. Win, "A mathematical model for wideband ranging," *IEEE J. Sel. Areas Commun.*, vol. 9, no. 2, pp. 216–228, 2015.

[17] A. Giorgetti and M. Chiani, "Time-of-arrival estimation based on information theoretic criteria," *IEEE Trans. Signal Process.*, vol. 61, no. 8, pp. 1869–1879, 2013.

[18] Z. Yin, Z. Wang, X. Liu, and Z. Wu, "Design of pulse waveform for waveform division multiple access uwb wireless communication system," *The scientific world journal*, vol. 2014, no. 5, p. 171875, 2014.

[19] Z. Yin, K. Cui, Z. Wu, and L. Yin, "Entropy-based toa estimation and svm-based ranging error mitigation in uwb ranging systems," *Sensors*, vol. 15, no. 5, pp. 11701–11724, 2015.

[20] Z. Yang, J. Deng, and A. Nallanathan, "Moving target recognition based on transfer learning and three-dimensional over-complete dictionary," *IEEE Sensors J.*, vol. 16, no. 14, pp. 1–1, 2016.

[21] J. Deng, Z. Zhang, E. Marchi, and B. Schuller, "Sparse autoencoder-based feature transfer learning for speech emotion recognition," in *Proc. ACII'13*, pp. 511–516, IEEE, 2013.

[22] Y. Bengio, A. Courville, and P. Vincent, "Representation learning: A review and new perspectives," *IEEE Trans. Pattern Anal. Mach. Intell*, vol. 35, no. 8, pp. 1798–1828, 2013.

[23] Y. Bengio, "Deep learning of representations for unsupervised and transfer learning," *Unsupervised and Transfer Learning Challenges in Machine Learning*, vol. 7, p. 19, 2012.

[24] J. Deng, R. Xia, Z. Zhang, Y. Liu, and B. Schuller, "Introducing shared-hidden-layer autoencoders for transfer learning and their application in acoustic emotion recognition," in *Proc. ICASSP'14*, pp. 4818–4822, IEEE, 2014.